

# Acylootropic Tautomerism: XXXV.\* $R \rightleftharpoons L$ -Inversion of Configuration of Dipolar Spirocyclic and Open-Chain 2-Arylamino tropone Isomers

L. P. Olekhovich<sup>1</sup>, Z. N. Budarina<sup>2</sup>, G. S. Borodkin<sup>2</sup>, S. V. Kurbatov<sup>1</sup>,  
G. S. Vaslyayeva<sup>1</sup>, and Yu. A. Zhdanov<sup>1</sup>

<sup>1</sup> Rostov State University, ul. Zorge 7, Rostov-on-Don, 344090 Russia

<sup>2</sup> Research Institute of Physical and Organic Chemistry, Rostov State University,  
pr. Stachki 194/3, Rostov-on-Don, 344104 Russia

Received June 21, 2000

**Abstract**— $R \rightleftharpoons L$ -Inversion of chiral spirocyclic and open-chain 2-arylamino tropone derivatives with varied heteroatom (O, S, N) has been studied. Kinetic relations holding in the  $R, L$ -permutation are discussed. Its mechanism includes formation and dissociation of spiro bonds and torsion stereodynamics.

Using the dynamic NMR technique, we recently [2] revealed degenerate  $R \rightleftharpoons L$ -inversion (Scheme 1) of chiral spiro  $\sigma$ -complexes like **Ia**, which are stable intermediates in intramolecular acylootropic tautomerism  $\mathbf{Ib} \rightleftharpoons \mathbf{Ib}'$  [1, 3–5]. This process is analogous to bimolecular nucleophilic substitution reactions at the *ipso*-carbon atom ( $C^*$ ) of electron-deficient arenes [6]. With the goal of studying kinetic features of the  $R \rightleftharpoons L$  process we have synthesized a series of new compounds **II–VII** (see Experimental) containing various nitroaryl fragments **A–D** (Scheme 2) and heteroatoms X (O, S, NR) in the aminotropone fragment. Spirocyclic isomers **a** of compounds **I–VII** have zwitterionic structure due to delocalization of the positive charge in the tropylium fragment, and of the negative, over the nitroaryl moiety (Schemes 1 and 2). These isomers are insoluble in weakly polar media, so that the corresponding NMR experiments were carried out mainly with their solutions in  $C_6D_5NO_2$  and DMSO- $d_6$ .

The  $^1H$  NMR spectra of spiro compounds **IIA–VA** are characterized by a considerable upfield shift of the doublet  $6'-H$  signal of the dinitroaryl fragment

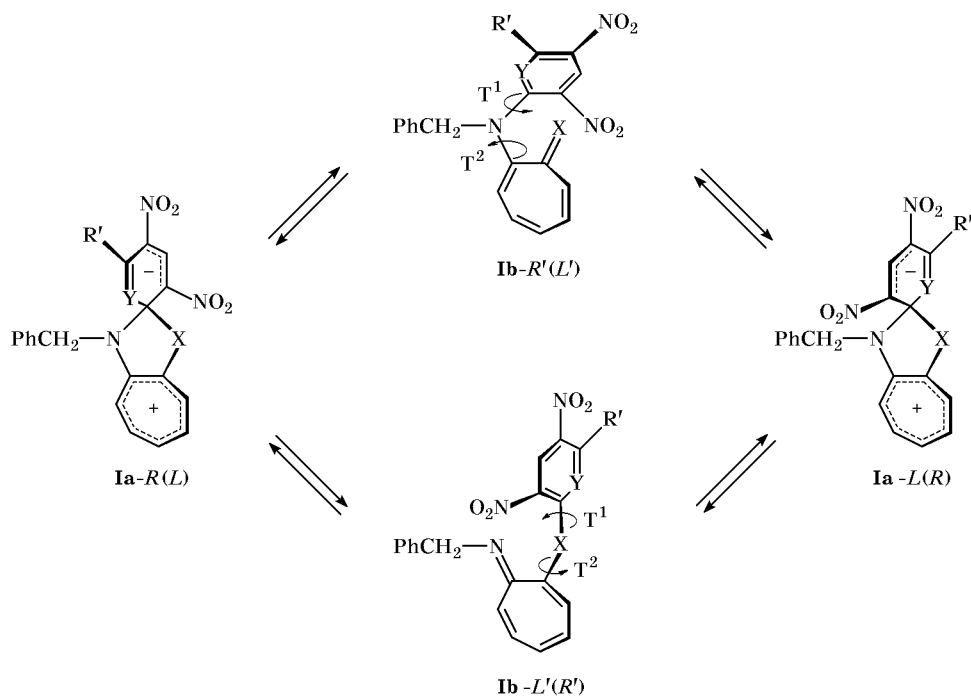
( $\delta$  5.7–5.9 ppm; Fig. 1a). This indicates that  $\pi$ -orbitals of  $C^{5'}$  and  $C^{6'}$  do not participate in delocalization of the negative charge and that the corresponding double bond is vinyl-like (structure **A** in Scheme 2). An analogous C=N fragment in 3,5-dinitropyridyl was revealed [5] by X-ray analysis of spirocyclic compound derived from 3,5-dinitropyridine and  $N, N'$ -dimethyl-2-amino-2,4,6-cycloheptatrieneimine (structure **B** in Scheme 2).

Figure 1b shows the evolution with temperature of the  $AB$  quartet from the  $N$ -benzyl  $CH_2$  group of compound **VA**, which can be regarded as diastereotopic indicator of  $R, L$ -conversion [2, 7]. The kinetic and activation parameters of the  $R, L$ -conversion for compounds **II–VII** were determined by computer simulation of the shape of reference signals (Table 1). It is seen that the  $R, L$ -conversion rate varies over a very wide range, from extremely slow for compounds **IID**, **IVD**, and **VD** to fairly fast for **VID** and **VIIB**. Let us compare the data given in Table 1 for aminotropone imine derivatives **IIA–VA**, **IIB**, **IID**, **IVD**, and **VD** with those of aminotropone **VID** and aminothio tropones **VIIB–VIID**. First, spirocyclic compounds **IIA–VA**, **IIB**, **IID**, **IVD**, and **VD**, unlike their oxygen and sulfur analogs ( $X = O, S$ ) are characterized by a high barrier to  $L \rightleftharpoons R$ -inversion. Second, fusion of a benzene ring to fragment **A** strongly suppresses inversion (compounds **IID**, **IVD**, and **VD**; Table 1). When their solutions were heated up to 180–200°C, we observed in the  $^1H$  NMR spectra only uniform

\* For communication XXXIV, see [1].

\*\* This study was financially supported by the Russian Foundation for Basic Research (project no. 99-03-33496a) and by the Program “Universities of Russia. Basic Research at Higher School in the Field of Natural Science and Humanities” (project no. 991440).

Scheme 1.



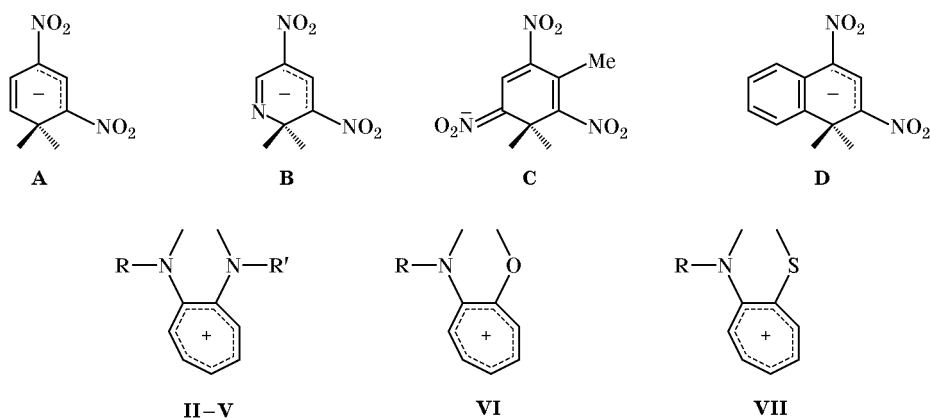
signal broadening and no collapse of the *AB*-quartet from the CH<sub>2</sub>Ph group (Fig. 1c), which is typical of the other compounds (Fig. 1b).

An analogous pattern is observed on variation of substituent on the nitrogen atom in **II–V**. The *R* ⇌ *L*-conversion of **IIA–VA** is strongly accelerated (by more than two orders of magnitude; Table 1) on replacement of *N*-isopropyl or *N*-benzyl group by bulkier *N*-*tert*-butyl group. The same replacement in the series **IID**, **IVD**, and **VD** does not reduce the activation threshold for *R,L*-dynamics (Fig. 1c,

Table 1). However, in going from **IID**, **IVD**, and **VD** to oxygen and sulfur analogs **VID** and **VIIID** the rate of the *R,L*-process increases very sharply, by a factor of more than 10<sup>10</sup>–10<sup>13</sup>; Table 1). This means that benzene ring fusion does not suppress *R,L*-conversion of the troponone and thiotroponone derivatives.

The presence of a methyl group in position 3 of the 2,4,6-trinitrophenyl fragment (structure **C** in Scheme 2) promotes torsions of the neighboring nitro groups (in positions 2 and 4); therefore, the degree of their participation in  $\pi$ -delocalization of the negative

Scheme 2.



**II**, R = R' = CH<sub>2</sub>Ph; **III**, R = R' = *i*-Pr; **IV**, R = CH<sub>2</sub>Ph, R' = *i*-Pr; **V**, R = CH<sub>2</sub>Ph, R' = *t*-Bu; **VI**, **VII**, R = CH<sub>2</sub>Ph.

**Table 1.** Kinetic and activation parameters of the  $R \rightleftharpoons L$ -permutation of arylaminotropone derivatives **II–IV**

| Compound no. | Solvent                                       | $k_{298}$ , s <sup>-1</sup> | $\Delta H^\ddagger$ , kJ/mol | $\Delta S^\ddagger$ , J mol <sup>-1</sup> K <sup>-1</sup> | $\Delta G_{298}^\ddagger$ , kJ/mol | Temperature range, K |
|--------------|---|-----------------------------|------------------------------|---|------------------------------------|----------------------|
| <b>IID</b>   | C <sub>6</sub> D <sub>5</sub> NO <sub>2</sub> | <10 <sup>-9</sup>           | –                            | –   | >125.4                             | 313–473              |
|              | DMSO- <i>d</i> <sub>6</sub>                   | <10 <sup>-9</sup>           | –                            | –   | >125.4                             | 313–453              |
| <b>IVD</b>   | C <sub>6</sub> D <sub>5</sub> NO <sub>2</sub> | <10 <sup>-9</sup>           | –                            | –   | >125.4                             | 313–473              |
|              | DMSO- <i>d</i> <sub>6</sub>                   | <10 <sup>-9</sup>           | –                            | –   | >125.4                             | 313–453              |
| <b>VD</b>    | C <sub>6</sub> D <sub>5</sub> NO <sub>2</sub> | <10 <sup>-9</sup>           | –                            | –   | >125.4                             | 313–473              |
| <b>IIA</b>   | C <sub>6</sub> D <sub>5</sub> NO <sub>2</sub> | 4.46 × 10 <sup>-1</sup>     | 45.57 ± 0.59                 | -104.08 ± 1.38  | 77.58                              | 313–433              |
|              | DMSO- <i>d</i> <sub>6</sub>                   | 2.80 × 10 <sup>-3</sup>     | 94.47 ± 0.46                 | 23.83 ± 1.17  | 87.36                              | 313–433              |
| <b>IIIA</b>  | C <sub>6</sub> D <sub>5</sub> NO <sub>2</sub> | 2.29 × 10 <sup>-2</sup>     | 82.72 ± 0.46                 | 11.88 ± 1.30  | 82.18                              | 313–353              |
|              |   | 1.83 × 10 <sup>-3</sup>     | 122.89 ± 0.54                | 115.66 ± 1.42   | 88.41                              | 353–433              |
| <b>IVA</b>   | C <sub>6</sub> D <sub>5</sub> NO <sub>2</sub> | 2.30 × 10 <sup>-2</sup>     | 82.14 ± 0.50                 | 0.00 ± 1.12   | 82.14                              | 313–373              |
|              |   | 5.08 × 10 <sup>-5</sup>     | 157.29 ± 0.54                | 201.48 ± 1.13   | 97.27                              | 373–433              |
|              | DMSO- <i>d</i> <sub>6</sub>                   | 3.86 × 10 <sup>-3</sup>     | 87.19 ± 0.42                 | 2.09 ± 1.05   | 86.57                              | 323–433              |
| <b>VA</b>    | C <sub>6</sub> D <sub>5</sub> NO <sub>2</sub> | 3.29                        | 72.65 ± 0.46                 | 9.20 ± 1.09   | 69.89                              | 293–413              |
| <b>IIB</b>   | C <sub>6</sub> D <sub>5</sub> NO <sub>2</sub> | 2.0 × 10 <sup>-2</sup>      | 43.47 ± 0.50                 | -131.25 ± 1.05  | 83.14                              | 323–433              |
|              | DMSO- <i>d</i> <sub>6</sub>                   | 1.1 × 10 <sup>-2</sup>      | 52.33 ± 0.46                 | -104.50 ± 1.05  | 88.32                              | 323–433              |
| <b>VIID</b>  | C <sub>6</sub> D <sub>5</sub> NO <sub>2</sub> | 56.3                        | 77.46 ± 0.75                 | 48.91 ± 1.92  | 62.87                              | 293–373              |
|              | DMSO- <i>d</i> <sub>6</sub>                   | 3.34                        | 80.76 ± 0.88                 | 36.66 ± 2.05  | 69.85                              | 293–393              |
| <b>VID</b>   | CDCl <sub>3</sub>                             | 1.2 × 10 <sup>3</sup>       | 46.11 ± 1.42                 | -29.51 ± 3.43   | 55.26                              | 213–313              |
|              | (CD <sub>3</sub> ) <sub>2</sub> CO            | 9.2 × 10 <sup>2</sup>       | 48.11 ± 0.30                 | -26.92 ± 3.26   | 56.05                              | 213–303              |
| <b>VIIC</b>  | CD <sub>3</sub> CN                            | 6.29 × 10 <sup>3</sup>      | 51.21 ± 0.96                 | 0.00 ± 2.01   | 51.21                              | 223–313              |
| <b>VIIIB</b> | C <sub>6</sub> D <sub>5</sub> NO <sub>2</sub> | 1.13 × 10 <sup>2</sup>      | 61.15 ± 0.67                 | 0.00 ± 1.71   | 61.15                              | 278–338              |
|              | DMSO- <i>d</i> <sub>6</sub>                   | 64.5                        | 55.97 ± 0.59                 | -23.41 ± 1.34   | 62.53                              | 293–363              |

charge decreases, and stabilization of the spiro isomer of **VIIC** (**a**) weakens. Obviously, this is the reason why the  $R,L$  conversion of **VIIC** is characterized by the highest rate (Table 1).

The  $R \rightleftharpoons L$  process includes three steps, two of which require some energy (Scheme 1): dissociation of the C\*–X bond (X = N, O, S), which accompanies the transition from spiro isomers **a** or **a'** to open-chain isomers **b** or **b'**; proper  $R,L$ -conversion **b**- $R' \rightleftharpoons b$ - $L'$  (**b'- $L' \rightleftharpoons b'$ - $R'$ ) of isomers **b** via torsions about the arene–X ( $T^1$ ) and tropone–X bonds ( $T^2$ ); and cyclization to give inverted spiro structure.**

In order to interpret the observed kinetic relations in the  $R,L$ -conversion of compounds **II–VII**, the following questions should be answered: (1) What is the geometry of the five-membered reactive entity in the primary elementary step (dissociation of the C\*–X bond): is it planar ( $P$ ) or envelope-like ( $E$ )? (2) What bond, C\*–N, C\*–O, or C\*–S in oxygen and sulfur derivatives is cleaved first? (3) Does fusion of a benzene ring affect the strength of the spiro bonds? (4) What are the contributions of spiro bond dissociation and torsions  $T^1$  and  $T^2$  to the overall  $R,L$ -inversion barrier?

Scheme 3 shows that the primary act, cleavage of the C\*–X bond, requires either planar ( $P$ ) or envelope ( $E^a$ ,  $E^s$ ; the superscript  $s$  stands for *syn*, and  $a$ , for *anti*) geometry of the five-membered entity. Conformation  $E^a$  is possible for spiro compounds **IIA–VIIA** and **IIB**, whereas conformation  $E^s$  for all compounds **II–VII** is unfavorable because of steric repulsion between the tropylium ring and NO<sub>2</sub> group in the *ortho*-position of the arene moiety. For compounds having a dinitronaphthalene fragment (**D**),  $E^a$  conformer is also unfavorable (Scheme 3). Clearly, if cleavage of the spiro bond is possible only when the reactive entity has envelope-like geometry ( $E$ ),  $R,L$ -enantiomerism of **IID**, **IVD**, and **VD** would be suppressed. If planar geometry is necessary (Schemes 1 and 3), other, less obvious reasons for suppression of the  $R,L$ -conversion should be sought for.

Using the PM3 method, we calculated the heats of formation ( $H_f$ ) of model anionic  $\sigma$ -complexes **VIIa** and **IXa** and transition states **b** for their dissociation (Scheme 4). The difference between  $H_f(\mathbf{a})$  and  $H_f(\mathbf{b})$  ( $\Delta H_f$  in Table 2) corresponds to the energy of activation for dissociation of the C\*–X bond. Table 3 contains  $H_f$  values for spirocyclic and open-chain isomers

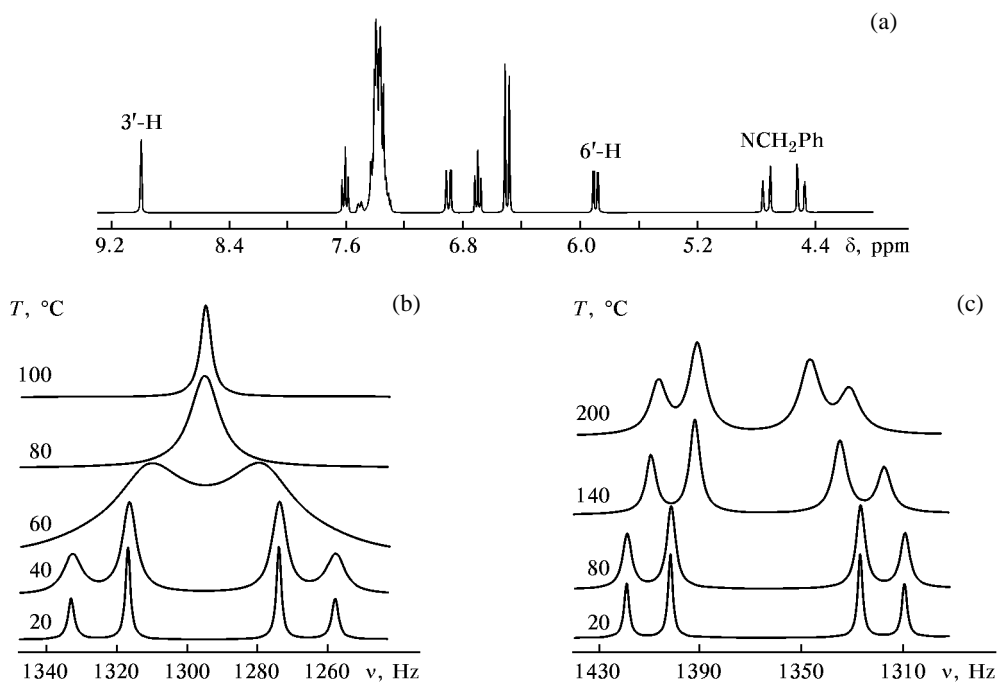


**Fig. 1.** (a)  $^1\text{H}$  NMR spectrum (25°C) of spiro isomer **VA** and temperature evolution of the *AB*-quartet from the *N*-benzyl  $\text{CH}_2$  group of (b) compound **VA** and (c) **VD**.

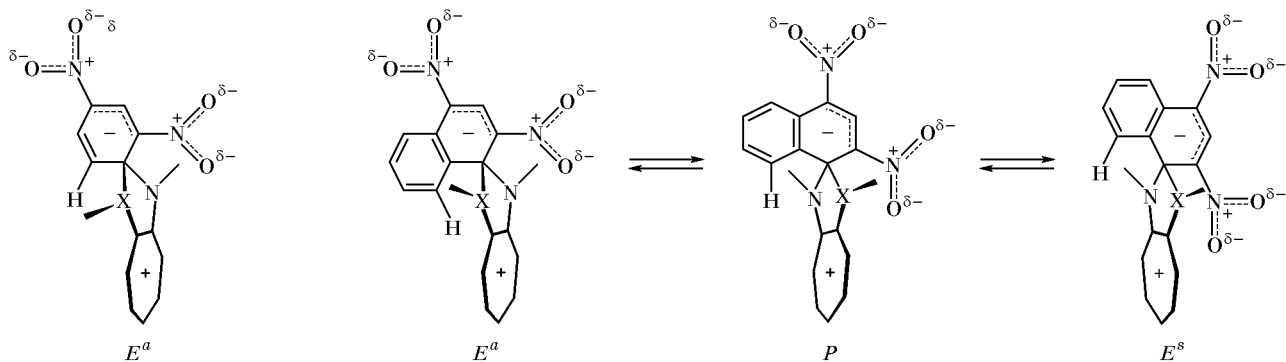
of compounds **II–VII** (Schemes 1 and 5) and activation barriers  $\Delta H_f$  to cleavage of the  $\text{C}^*-\text{X}$  bond (in the calculations,  $\text{NCH}_2\text{Ph}$  and  $\text{NPr}_i$  fragments were replaced by  $\text{NMe}$  group).

The calculated activation barriers (Table 2) to  $\text{C}^*-\text{X}$  bond cleavage in anionic  $\sigma$ -complexes **VIII** and **IX** are much higher than for spiro compounds **II–VII** (Table 3). This difference is determined by the nature of the leaving group  $\text{X}$ . In compounds **VIIIb** and **IXb** (Scheme 4)  $\text{X}$  is an anion ( $\text{NH}_2^-$ ,  $\text{HO}^-$ ,  $\text{HS}^-$ ); however,  $\text{X}$  is a neutral species in structures **b** of **II–IV**, where it goes away as a part of imino, keto, or thioketone group (Scheme 1). The activation energy  $\Delta H_f$  of the elementary step **VIIIa**, **Xa**  $\rightarrow$  **VIIIb**, **IXb**

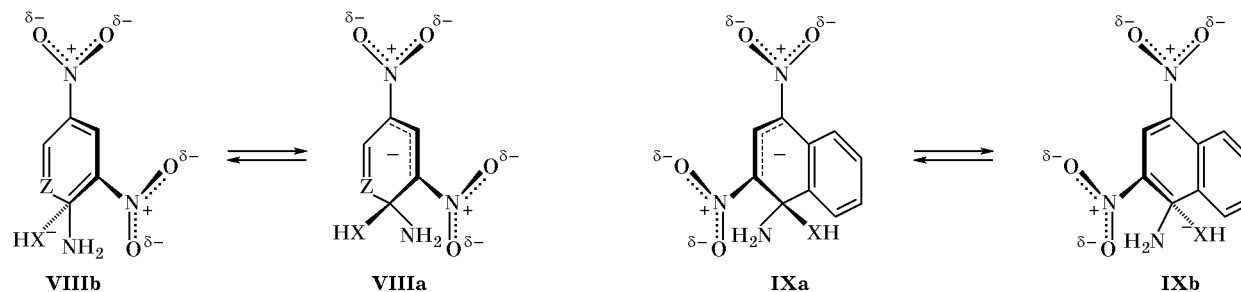
(Scheme 4) decreases in the series  $\text{X} = \text{N} > \text{O} \gg \text{S}$  (Table 2). Compounds **II–VII** give rise to the reverse  $\Delta H_f$  series:  $\text{S} \geq \text{N} > \text{O}$  (Table 3). Obviously, *R,L*-conversion in the aminotroponone derivatives involves preferential cleavage of the  $\text{C}^*-\text{O}$  bond, and in the aminothioproponone compounds, the  $\text{C}^*-\text{N}$  bond.

According to the calculations of transition states for  $\text{C}^*-\text{X}$  bond cleavage, the five-membered reactive entity in **II–VII** is planar (Scheme 5); therefore, the difference in size of the arene fragments could not affect this process. Also, fusion of a benzene ring in anionic  $\sigma$ -complexes **VIIIa** and **IXa** does not change the activation barriers  $\Delta H_f$  to  $\text{C}^*-\text{X}$  bond cleavage (Table 2); as concerns compounds **II–VII**,  $\Delta H_f$

**Scheme 3.**

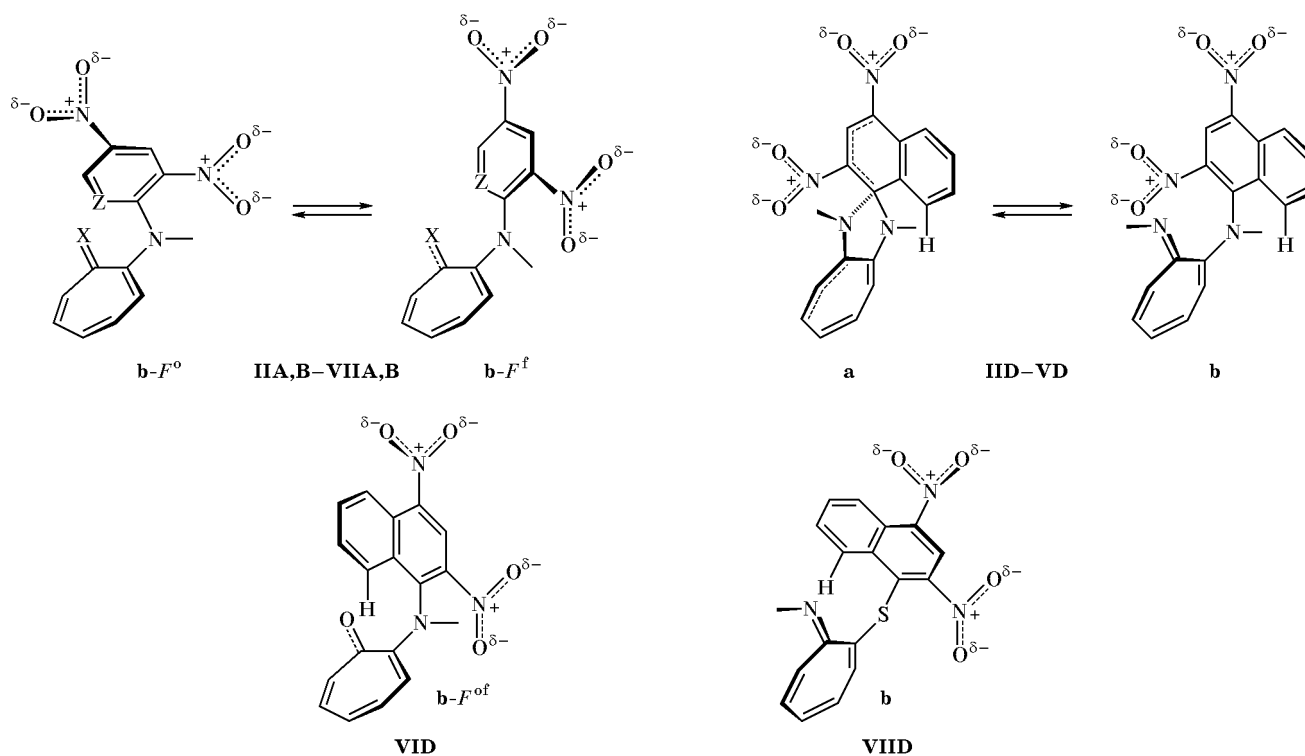


Scheme 4.



**VIII**, X = NH, Z = CH; X = O, Z = CH; X = S, Z = CH; X = NH, Z = N; X = O, Z = N; X = S, Z = N; **IX**, X = NH, O, S.

Scheme 5.



increases by only 6.3–8.4 kJ/mol (Table 3). Such a gain is clearly insufficient to suppress *R,L*-conversion so strongly as it is observed experimentally ( $\Delta\Delta G^\ddagger \geq 42$  kJ/mol; Fig. 1c, Table 1).

Now let us consider the stereodynamics of torsions  $T^1$  and  $T^2$  which are in fact responsible for the *R,L*-conversion (Scheme 1) following the  $C^*-X$  bond cleavage. We previously found [8] that *N*-aryl(hetaryl) derivatives of aminotropone like **VIA** and **VIB** do not form spiro isomers **a**, but their open-chain isomers **b** are *R',L'*-chiral (Schemes 1 and 5), and their inversion through conjugate  $T^1, T^2$  torsions are characterized by activation barriers of 45.1 to 46.8 kJ/mol.

Benzene ring fusion increases the activation barrier to *R,L*-conversion for compound **VID** by 4.2 kJ/mol (Table 1), and for its thio analog **VIID**, by 12.5–20.9 kJ/mol relative to trinitro compound **VIIC**. However, unlike aryl(hetaryl) aminotropone derivatives **VIA** and **VIB** [8] and compound **VIIC**, naphthalene derivatives **VID** and **VIID** give rise to ring-chain isomerism **a**  $\rightleftharpoons$  **b**; spiro isomer **a** of **VIID** prevails in the equilibrium mixture (Fig. 2). Obviously, energy consumption for cleavage of the  $C^*-N$  bond in spiro isomers rather than hindrance to  $T^1$  torsion of the naphthalene system is the main factor determining increased activation barrier to *R,L*-conversion in

**Table 2.** Calculated (PM3) activation energies for C\*–X bond cleavage in model anionic  $\sigma$ -complexes **VIII** and **IX**

| $\sigma$ -Complex no.    | Activation energy $E_a$ ( $\Delta H_f$ , kJ/mol) for cleavage of the C*–X bond |            |            |            |            |
|--------------------------|--|------------|------------|------------|------------|
|                          | NN (X = N)   | ON (X = O) | ON (X = N) | SN (X = S) | SN (X = N) |
| <b>VIII</b> <sup>a</sup> | 270.03   | 227.81     | 431.79     | 75.24      | 390.83     |
| <b>VIII</b> <sup>b</sup> | 273.79   | 249.55     | 441.41     | 91.12      | 396.68     |
| <b>IX</b>                | 261.25   | 228.23     | 428.45     | 88.62      | 387.90     |

<sup>a</sup> X = NH, Z = CH; X = S, Z = CH.<sup>b</sup> X = NH, Z = N; X = S; Z = N.**Table 3.** Calculated (PM3) heats of formation ( $H_f$ , kJ/mol) of spiro  $\sigma$ -complexes **IIa–VIIa** and open-chain conformers **IIb–VIIb** and energies of transition states ( $\Delta H_f$ , kJ/mol) for C\*–X bond cleavage<sup>a</sup>

| Compound no.                | NO                  | $\Delta H_f$ | NS               | $\Delta H_f$ | NN              | $\Delta H_f$ |
|-----------------------------|---------------------|--------------|------------------|--------------|-----------------|--------------|
| <b>VIA-a, VIIA-a, IIA-a</b> | 212.55              |              | 420.84           |              | 334.15          |              |
| <b>VIA-b, VIIA-b, IIA-b</b> | (N) 235.25          | 22.70        | (N) 446.22       | 25.33        | (N) 387.74      | 53.59        |
|                             | (O) 234.50          | 21.95        | (S) 475.52       | 53.73        | $F^o$ 203.78    |              |
|                             | $F^o$ (N) 203.78    |              | $F^o$ (N) 395.22 |              | $F^f$ 165.57    |              |
|                             | $F^o$ (O) 165.57    |              | $F^f$ (N) 405.21 |              |                 |              |
| <b>VID-a, VIID-a, IID-a</b> | 290.72              |              | 510.63           |              | 423.56          |              |
| <b>VID-b, VIID-b, IID-b</b> | (N) 324.41          | 8.06         | (N) 540.89       | 30.26        | (N) 480.11      | 56.56        |
|                             | (O) 320.94          | 7.23         | (S) 571.11       | 61.32        | 470.79          |              |
|                             | $F^o$ (N) 262.75    |              | (N) 510.04       |              | $F^{of}$ 478.86 |              |
|                             | $F^{of}$ (O) 165.57 |              |                  |              |                 |              |
| <b>VIB-a, VIIB-a, IIB-a</b> | 204.44              |              | 428.91           |              | 340.54          |              |
| <b>VIB-b, VIIB-b, IIB-b</b> | (N) 249.84          | 45.39        | (N) 470.84       | 42.34        | (N) 410.64      | 70.06        |
|                             | (O) 240.31          | 35.86        | (S) 502.56       | 73.65        | $F^o$ 369.85    |              |
|                             | $F^o$ (O) 178.07    |              | $F^o$ (N) 431.00 |              | $F^f$ 384.43    |              |
|                             |                     |              | $F^o$ (S) 483.50 |              |                 |              |

<sup>a</sup> The X atom is given in parentheses.

these compounds. Therefore, the energy of activation for  $T^{1,2}$ -torsions may be assumed to range from 46 to 54 kJ/mol for all compounds **I–VII**, both those for which the equilibrium **a**  $\rightleftharpoons$  **b** is displaced completely toward open-chain isomers **b** [8] and those stable in spiro form **a** [2].

It is still impossible to estimate in terms of the PM3 procedure the energy of activation of  $T^1$  and  $T^2$  torsions because of their concerted conjugation [8] in isomers **b** of **II–VII**. Unlike Hessians of transition states for a single elementary step, cleavage of spiro-C\*–X bonds, Hessians of transition conformers for open-chain isomers **b** are characterized by two vibrations with negative frequencies corresponding to  $T^{1,2}$ -torsions. However, the known algorithms [9] allow energy minimization of transition states to be performed for only one elementary act (either  $T^1$  or  $T^2$ ).

Nevertheless, the state of ring–chain equilibrium **a**  $\rightleftharpoons$  **b** (Scheme 1) for each compound of the series **II–VII** can be estimated by comparing the calculated  $H_f$  values for spirocyclic isomer **a** and open-chain conformers **b** (Scheme 5) corresponding to global or local minima on the potential energy surface.

As follows from the data in Table 3, open-chain isomers **b** of compounds **II–VII** having a 2,4-dinitrophenyl (**A**) and 3,5-dinitropyridyl moieties (**B**) (Scheme 2) exist mainly as flagpole ( $F$ ) conformations with an orthogonal ( $F^o$ ) or frontal ( $F^f$ ) mutual orientation of the arene and tropone moieties (Scheme 5). Fusion of a benzene ring makes  $F$ -conformers unfavorable: “hybrid”  $F^{of}$ -conformation of isomer **b** is still feasible for compound **VID**, but all these ( $F^o$ ,  $F^f$ , and  $F^{of}$ ) are thermodynamically unfavorable (Table 3) for open-chain isomers of **IID–VD** and **VIIG**. The

$R \rightleftharpoons L$  inversion ( $T^{1,2}$ ) in **IIA, B–VIIA, B** begins after relaxation of transition states for  $C^*-X$  bond cleavage to  $F$ -conformers; but for naphthalene derivatives **IID, IVD, VD, and VID** the inversion process directly follows the  $C^*-X$  bond cleavage (Scheme 5).

From comparison of the experimental (Table 1; Figs. 1, 2) and calculated data (Table 3) it follows that the  $R \rightleftharpoons L$ -dynamics in the series of compounds **II–VII** can formally be represented as potential energy surface sections shown in Fig. 3. Figure 3a illustrates the situation when spirocyclic isomers **a** occupy local minima, and their open-chain isomers **b** appear in global minima. An alternative state of the equilibrium  $a \rightleftharpoons b$  is given in Fig. 3b. The PES section shown in Fig. 3c looks like a “funnel” with compounds **IID, IVD, VD** at the bottom; this section clearly illustrates inhibition of the  $R, L$ -inversion. Open-chain isomers **b** of **IID, IVD, and VD** do not populate effectively the corresponding areas on the PES, for their heats of formation ( $\Delta H_f = 1.2$ – $9.2$  kJ/mol; Table 3) are comparable with the energies of transition states for  $C^*-N$  bond cleavage (Scheme 5).

As noted above, the activation energies for  $T^{1,2}$ -dynamics of open-chain isomers of all compounds **II–VII** fall into a narrow range ( $\sim 46$ – $54$  kJ/mol). The calculated geometries of compounds **IID–VD** and **VII G** are similar (Scheme 5) both in transition states corresponding to extension of the  $C^*-X$  bond ( $r = \sim 2.07, 1.92$  Å) and after its cleavage ( $r = \sim 2.57, 2.75$  Å) when  $T^{1,2}$  torsions (proper  $R \rightleftharpoons L$ -conversion) become possible. Just the difference in the heats of formation (Table 3) of isomers **b** is responsible for suppression of  $R, L$ -dynamics in **IID, IVD, and VD** ( $\Delta G^\ddagger \geq 125.4$  kJ/mol) and for the reverse situation with compound **VII D** ( $\Delta G^\ddagger = 68.6$  kJ/mol; Table 1).

Thus the overall activation barrier to  $R, L$ -permutation of **IID, IVD, and VD** is high since it includes energy expenses for both cleavage of the spiro bond and  $T^{1,2}$  torsions (Fig. 3c). In the  $R \rightleftharpoons L$ -conversion of **IIA–VA, IIB, and VII D**, the activation barrier to  $T^{1,2}$ -torsions is increased only by the energy difference (Table 3) between states **a** and **b** (Fig. 3b). The  $R', L'$ -permutation of **VID** and **VII C** depends only on the energy of  $T^{1,2}$ -dynamics in  $F$ -conformers of their stable isomers **b** (Fig. 3a; Scheme 5).

## EXPERIMENTAL

The dynamic  $^1H$  NMR spectra were recorded on a Varian VXR-300 spectrometer (300 MHz) (Table 1). The electron absorption spectra were measured on a Specord UV-Vis instrument in toluene and DMSO. The rate constants for  $R, L$ -permutation were deter-

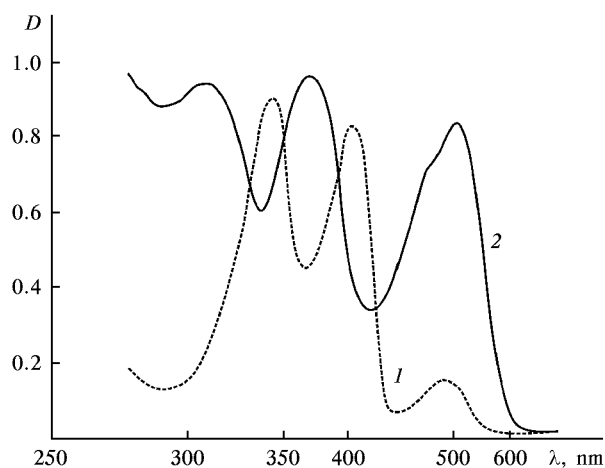


**Fig. 2.** Electron absorption spectra of compounds (1) **VID** and (2) **VII D** in DMSO ( $c = 5 \times 10^{-5}$  M).

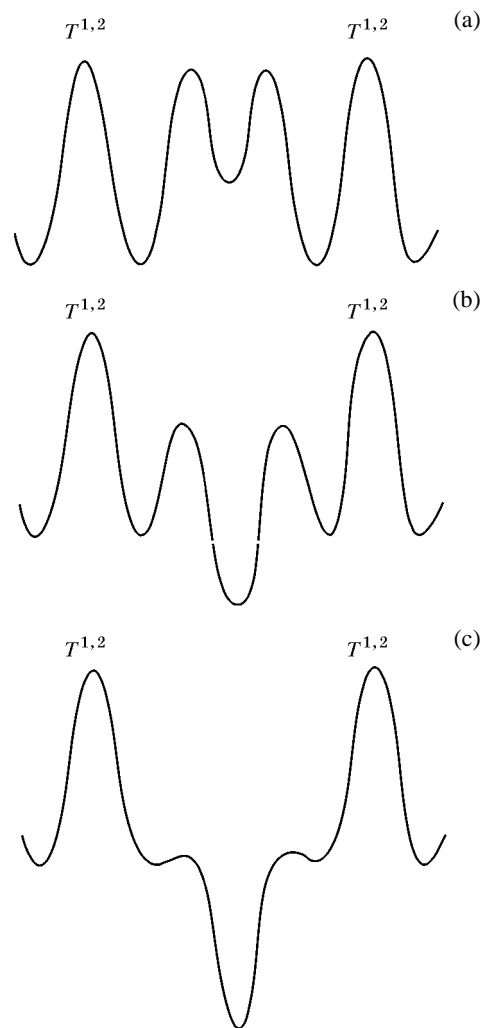


**Fig. 3.** Potential energy surface sections corresponding to  $R, L$ -permutation of (a) compounds **VID, VII B, and VII C**; (b) **IIA–VA, IIB, and VII D**; and (c) **IID, IVD, and VD**.

**Table 4.** Melting points, yields, and elemental analyses of compounds **II–VII**

| Comp. no.               | mp, °C (solvent)         | Yield, % | Found, % |      |       | Formula   | Calculated, % |      |       |
|-------------------------|--------------------------|----------|----------|------|-------|---|---------------|------|-------|
|                         |                          |          | C        | H    | N     |   | C             | H    | N     |
| <b>IIA</b>              | 235 (CHCl <sub>3</sub> ) | 65       | 69.15    | 4.45 | 12.30 | C <sub>27</sub> H <sub>22</sub> N <sub>4</sub> O <sub>4</sub>   | 69.52         | 4.75 | 12.01 |
| <b>IIIA</b>             | 265 (ethanol)            | 74       | 61.46    | 5.79 | 15.23 | C <sub>19</sub> H <sub>22</sub> N <sub>4</sub> O <sub>4</sub>   | 61.60         | 5.98 | 15.12 |
| <b>IVA</b>              | 220 (ethanol)            | 56       | 66.24    | 5.41 | 13.48 | C <sub>23</sub> H <sub>22</sub> N <sub>4</sub> O <sub>4</sub>   | 66.01         | 5.29 | 13.39 |
| <b>VA</b>               | 210 (ethanol)            | 70       | 66.43    | 5.37 | 12.68 | C <sub>24</sub> H <sub>24</sub> N <sub>4</sub> O <sub>4</sub>   | 66.65         | 5.59 | 12.95 |
| <b>IIB</b>              | 260 (benzene)            | 76       | 66.44    | 4.69 | 14.67 | C <sub>26</sub> H <sub>21</sub> N <sub>5</sub> O <sub>4</sub>   | 66.80         | 4.53 | 14.98 |
| <b>IID</b>              | 290 (ethanol)            | 90       | 71.84    | 4.21 | 10.71 | C <sub>31</sub> H <sub>24</sub> N <sub>4</sub> O <sub>4</sub>   | 72.08         | 4.68 | 10.85 |
| <b>IVD</b>              | 270 (ethanol)            | 66       | 69.36    | 5.28 | 12.17 | C <sub>27</sub> H <sub>24</sub> N <sub>4</sub> O <sub>4</sub>   | 69.21         | 5.16 | 11.96 |
| <b>VD</b>               | 280 (ethanol)            | 78       | 69.53    | 5.21 | 11.48 | C <sub>28</sub> H <sub>26</sub> N <sub>4</sub> O <sub>4</sub>   | 69.61         | 5.43 | 11.61 |
| <b>VID</b>              | 160 (ethanol)            | 94       | 70.28    | 4.21 | 10.14 | C <sub>24</sub> H <sub>17</sub> N <sub>3</sub> O <sub>5</sub>   | 70.06         | 4.16 | 10.21 |
| <b>VIIB<sup>a</sup></b> | 150                      | 70       | 57.93    | 3.68 | 14.37 | C <sub>19</sub> H <sub>14</sub> N <sub>4</sub> O <sub>4</sub> S | 57.86         | 3.57 | 14.21 |
| <b>VIIC<sup>b</sup></b> | 175                      | 80       | 56.53    | 3.72 | 12.54 | C <sub>21</sub> H <sub>16</sub> N <sub>4</sub> O <sub>6</sub> S | 55.74         | 3.56 | 12.38 |
| <b>VIID<sup>c</sup></b> | 210                      | 92       | 65.19    | 3.61 | 9.64  | C <sub>24</sub> H <sub>17</sub> N <sub>3</sub> O <sub>4</sub> S | 65.00         | 3.86 | 9.48  |

<sup>a</sup> Found S, %: 8.25; calculated S, %: 8.13.

<sup>b</sup> Found S, %: 7.21; calculated S, %: 7.08.

<sup>c</sup> Found S, %: 7.07; calculated S, %: 7.23.

mined with an accuracy of  $\pm 10\%$  by computer simulation of signals from reference diastereotopic protons [8] and visual adjustment to the experimental signal shape at a given temperature. The activation parameters for *R,L*-dynamics (Table 1) were calculated by the standard linearization procedure ( $\ln k - 1/T$ ) with regression coefficients no less than 0.98.

Quantum-chemical calculations were performed using Hyper-Chem<sup>TM</sup> program kindly provided by Full Member of the Russian Academy of Sciences N.S. Zefirov and Prof. Yu.A. Ustynyuk.

The initial reactants, aryl halides, 1-fluoro-2,4-dinitronaphthalene, 1-chloro-3-methyl-2,4,6-trinitrobenzene, and the others, were synthesized by procedures analogous to those given in [10]; tropolone was prepared as described in [11].

**1,2-Diethoxytropylium tetrafluoroborate (I)** as starting compound for preparation of aminotropones was synthesized by improved procedure [12]. Tropolone sodium salt, 5 g, was added with stirring to a solution of 13.2 g of triethyloxonium tetrafluoroborate [13] in 20 ml of dry methylene chloride, cooled with an ice-salt bath. The mixture was kept for 12–16 h at room temperature and filtered, the precipitate was washed with methylene chloride on a filter, and the filtrate was poured into 200 ml of cold dry diethyl ether. The precipitate was filtered off, washed with ether on a filter, and recrystallized from ethanol. Yield 8 g (77%), mp 116°C; published data [12]: yield 63%, mp 115–116°C.

**1-Benzylamino-7-benzylimino-1,3,5-cycloheptatriene (II).** 1,2-Diethoxytropylium tetrafluoroborate, 1.6 g, was added in portions to 2 ml of benzylamine with stirring and cooling in an ice bath. A thick material was obtained, which was kept for 12–16 h at room temperature. It was diluted with water, and the precipitate was filtered off, washed with water, and dried in air. The product was purified by chromatography on Al<sub>2</sub>O<sub>3</sub> (eluent CHCl<sub>3</sub>), followed by recrystallization from ethanol. Yield 1.7 g (94%). Yellow crystals, mp 82°C; published data [14]: yield 90%, mp 82°C.

**1-Isopropylamino-7-isopropylimino-1,3,5-cycloheptatriene (III)** was synthesized in a similar way. The yellow product was recrystallized from methanol or light petroleum ether. Yield 80%, mp 66°C; published data [14]: yield 18%, bp 104–106°C (0.35 mm).

**7-Benzylimino-1-tert-butylamino-1,3,5-cycloheptatriene (V).** A mixture of 1 g of 2-benzylaminotroponone [15] and 2 g of freshly distilled dimethyl sulfate was heated to 110°C and was kept for 10 min at 110°C and for 12–16 h at room temperature. Excess dimethyl sulfate was removed by shaking with several 5-ml portions of benzene or toluene. 1-Benzylamino-2-methoxytropylium methyl sulfate thus obtained was dissolved in methanol, triethylamine was added until the mixture became alkaline, and 2 ml of *tert*-butylamine was added. The mixture was kept for several days at room temperature (until the reaction was complete, TLC), the precipitate was filtered off, the

Table 5.  $^1\text{H}$  NMR spectra of compounds II–VII<sup>a</sup>

| Compound no. | Solvent (temperature, °C)                          | $^1\text{H}$ NMR spectrum, $\delta$ , ppm ( $J$ , Hz)  |
|--------------|--|--|
| IIA          | DMSO- $d_6$ (20)                                   | 8.40 d (1H, 3'-H, $J_{3',5'} = 2.7$ ), 7.72–7.31 m (12H, $H_{\text{arom}}$ , 4-H, 6-H), 7.12 d.d (1H, 5''-H, $J_{5'',6''} = 8.3$ ), 7.01 t (1H, 5-H, $J_{5,6} = J_{4,5} = 8.6$ ), 6.88 d (2H, 3-H, 7-H, $J_{3,4} = J_{6,7} = 9.0$ ), 5.82 d (1H, 6''-H), 4.85–4.63 q (4H, 2CH <sub>2</sub> , $J_{\text{H,H}} = 17$ ) |
|              | DMSO- $d_6$ (160)                                  | 8.47 d (1H, 3'-H, $J_{3',5'} = 2.7$ ), 7.69–7.27 m (12H, $H_{\text{arom}}$ , 4-H, 6-H), 7.13 d.d (1H, 5''-H, $J_{5'',6''} = 8.3$ ), 7.01 t (1H, 5-H, $J_{5,6} = J_{4,5} = 8.6$ ), 6.92 d (1H, 3-H, 7-H, $J_{3,4} = J_{6,7} = 9.0$ ), 5.61 d (1H, 6'-H), 4.73 s (4H, 2CH <sub>2</sub> )                               |
| IIIA         | C <sub>6</sub> D <sub>5</sub> NO <sub>2</sub> (20) | 9.24 s (1H, 3'-H), 7.65 d.d (1H, 5'-H), 5.64 d (1H, 6'-H), 4.06 m [1H, CH(CH <sub>3</sub> ) <sub>2</sub> ], 1.59–1.46 q (6H, 2CH <sub>3</sub> , $J_{\text{H,H}} = 7$ )   |
| IVA          | DMSO- $d_6$ (20)                                   | 8.45 s (1H, 3'-H), 7.15 d.d (1H, 5'-H), 5.71 d (1H, 6'-H), 4.72–4.51 q (2H, CH <sub>2</sub> , $J_{\text{H,H}} = 17$ ), 3.76 m [1H, CH(CH <sub>3</sub> ) <sub>2</sub> ], 1.39–1.24 q (6H, 2CH <sub>3</sub> , $J = 7$ )  |
| VA           | C <sub>6</sub> D <sub>5</sub> NO <sub>2</sub> (20) | 9.09 s (1H, 3'-H), 7.3–7.4 m (2H, 5'-H, 6'-H), 4.82–4.60 q (1H, CH <sub>2</sub> , $J_{\text{H,H}} = 17$ ), 1.75 s (9H, 3CH <sub>3</sub> )  |
| IIID         | DMSO- $d_6$ (40)                                   | 8.81 s (1H, 3'-H), 4.72–4.39 q (2H, CH <sub>2</sub> , $J_{\text{H,H}} = 18$ )  |
| IVD          | DMSO- $d_6$ (40)                                   | 8.77 s (1H, 3'-H), 4.70–4.48 q (2H, CH <sub>2</sub> , $J_{\text{H,H}} = 17$ ), 3.89 m [1H, CH(CH <sub>3</sub> ) <sub>2</sub> ], 1.49–1.35 q (6H, 2CH <sub>3</sub> , $J = 7$ )  |
| VD           | DMSO- $d_6$ (40)                                   | 8.75 s (1H, 3'-H), 4.48–4.15 q (2H, CH <sub>2</sub> , $J_{\text{H,H}} = 17$ ), 1.2 s (9H, 3CH <sub>3</sub> )   |
| VII          | CDCl <sub>3</sub> (20)                             | 8.55 s (1H, 3'-H), 5.05 s (2H, CH <sub>2</sub> )   |
| VII B        | DMSO- $d_6$ (30)                                   | 8.48 s (1H, 3'-H), 8.4 s (1H, 5'-H), 5.28–5.0 collapsing q (2H, CH <sub>2</sub> )  |
| VII C        | CD <sub>3</sub> CN (20)                            | 8.42 s (1H, 3'-H), 5.0 s (2H, CH <sub>2</sub> ), 2.43 s (3H, CH <sub>3</sub> )   |
| VII D        | DMSO- $d_6$ (20)                                   | 8.83 s (1H, 3'-H), 4.89–4.64 q (2H, CH <sub>2</sub> , $J_{\text{H,H}} = 17$ )  |

<sup>a</sup> Signals from protons in the cycloheptatriene ring, phenyl ring of the *N*-benzyl group, and unsubstituted benzene ring in 2,4-dinitronaphthalene derivatives are similar for all compounds; therefore, they are given only for compound IIA.

filtrate was evaporated, and the residue was subjected to chromatography on Al<sub>2</sub>O<sub>3</sub> (eluent CHCl<sub>3</sub>). The solvent was removed from the eluate, and the residue was combined with the previously obtained precipitate and was recrystallized from light petroleum ether. Yield 66%. Light yellow crystals, mp 75°C.

**7-Benzylimino-1-isopropylamino-1,3,5-cycloheptatriene (IV)** was synthesized as described above for compound V by reaction of 1-benzylamino-2-methoxytropylium methyl sulfate with isopropylamine. Oily substance. Yield 60%.

**2-Benzylamino-2,4,6-cycloheptatrienethione (VII)**. To a solution of 2 g of 1-benzylamino-2-methoxytropylium methyl sulfate (see above) in 8 ml of ethanol we added with stirring 5 g of sodium sulfide and 20 ml of water in small portions. After 12–16 h, the precipitate was filtered off, washed with water, dried in air, and recrystallized from ethanol or methanol. Yield 89%. Orange crystals, mp 142°C; published data [14]: mp 138°C.

**2-Aminotropone imine and 2-aminotropone derivatives IIA,D–VA,D and VID**. A mixture of

1 mmol of 2-aminotropone imine (or 2-aminotropone), and 0.5 mmol of aryl halide (1-fluoro-2,4-dinitrobenzene or 1-fluoro-2,4-dinitronaphthalene) in 3 ml of chloroform was heated to the boiling point and was kept for 6–8 h at 70–80°C until the solvent was removed completely. The remaining melt was dissolved in chloroform and subjected to chromatography on Al<sub>2</sub>O<sub>3</sub>. The solution was evaporated, and the residue was washed with petroleum ether and recrystallized from ethanol. Spiro  $\sigma$ -complexes were isolated as bright red crystalline substances. Their melting points, yields, and elemental analyses are given in Table 4, and  $^1\text{H}$  NMR spectra, in Table 5.

**1,3-Dibenzyl-3'(5')-nitro-2,2',3,5'(3')-tetrahydro-1H-cyclohepta[d]imidazolium-2-spiro-2'-pyridine-5'(3')-nitronate (IIB)**. A solution of 1 mmol of 1-benzylamino-7-benzylimino-1,3,5-cycloheptatriene and 0.5 mmol of 2-chloro-3,5-dinitropyridine [16] in 5 ml of dry benzene was refluxed for 3 h. The mixture was filtered, the filtrate was evaporated, and the residue was subjected to chromatography on Al<sub>2</sub>O<sub>3</sub> using CHCl<sub>3</sub> as eluent. Yellow crystals, yield 76%.

**2-Benzylamino-2,4,6-cycloheptatrienethione derivatives VIIB–VIID.** A solution of 0.5 mmol of 2-benzylamino-2,4,6-cycloheptatrienethione, 0.25 mmol of aryl halide (2-chloro-3,5-dinitropyridine, 1-chloro-3-methyl-2,4,6-trinitrobenzene, or 1-chloro-2,4-dinitronaphthalene) in chloroform was applied to a plate with a layer of  $\text{Al}_2\text{O}_3$ . After 15–20 h, the  $\text{Al}_2\text{O}_3$ -immobilized mixture was transferred to a column charged with  $\text{Al}_2\text{O}_3$  to a height of about 7 cm. The column was eluted with chloroform, the eluate was evaporated, the residue was dispersed in a minimal amount of benzene, and the precipitate was filtered off and washed with benzene and diethyl ether. The yields, melting points, elemental analyses, and  $^1\text{H}$  NMR spectra of compounds **IIB** and **VIIB–VIID** are given in Tables 4 and 5.

## REFERENCES

- Kurbatov, S.V., Budarina, Z.N., Borisenko, N.I., Vaslyaeva, G.S., Knyazev, A.P., Olekhnovich, L.P., and Zhdanov, Yu.A., *Russ. J. Org. Chem.*, 1999, vol. 35, no. 11, pp. 1683–1688.
- Olekhnovich, L.P., Budarina, Z.N., Lesin, A.V., Kurbatov, S.V., Borodkin, G.S., and Minkin, V.I., *Mendeleev Commun.*, 1994, no. 2, pp. 162–165.
- Furmanova, N.G., Olekhnovich, L.P., Minkin, V.I., Struchkov, Yu.T., Kompan, O.E., and Budarina, Z.N., *Zh. Org. Khim.*, 1982, vol. 18, no. 3, pp. 474–484.
- Olekhnovich, L.P., Kurbatov, S.V., Budarina, Z.N., Minkin, V.I., and Zhdanov, Yu.A., *Zh. Org. Khim.*, 1985, vol. 21, no. 12, pp. 2550–2555.
- Kurbatov, S.V., Budarina, Z.N., Olekhnovich, L.P., Furmanova, N.G., Lesin, A.V., Kompan, O.E., Minkin, V.I., and Zhdanov, Yu.A., *Zh. Org. Khim.*, 1988, vol. 24, no. 5, pp. 913–922.
- Knyazev, V.N. and Drozd, V.N., *Russ. J. Org. Chem.*, 1995, vol. 31, no. 1, pp. 1–26; Terrier, F., *Chem. Rev.*, 1982, vol. 82, no. 2, pp. 77–152; Strauss, M.J., *Chem. Rev.*, 1970, vol. 70, no. 3, pp. 667–712.
- Eaton, S.S. and Holm, R.H., *Inorg. Chem.*, 1970, vol. 10, pp. 1446–1452.
- Olekhnovich, L.P., Kurbatov, S.V., Lesin, A.V., Budarina, Z.N., Zhdanov, Yu.A., and Minkin, V.I., *Zh. Org. Khim.*, 1991, vol. 27, no. 1, pp. 6–13.
- Tsai, C.J. and Jordan, K.D., *J. Phys. Chem.*, 1993, vol. 97, no. 8, pp. 1127–1137.
- Weygand–Hilgetag organisch-chemische Experimentierkunst*, Hilgetag, G. and Martini, A., Eds., Leipzig: Johann Ambrosius Barth, 1964, 3rd ed. Translated under the title *Metody eksperimenta v organicheskoi khimii*, Moscow: Khimiya, 1968, pp. 197, 230.
- Minus, R.A., Elliot, A.J., and Sheppard, W.A., *Org. Synth.*, 1977, vol. 57, no. 1, pp. 117–121.
- Forbes, C.E. and Holm, R.H., *J. Am. Chem. Soc.*, 1968, vol. 90, no. 12, p. 6884.
- Fieser, L.F. and Fieser, M., *Reagents for Organic Synthesis*, New York: Wiley–Intersci., vol. 1, 1967. Translated under the title *Reagenty dlya organicheskogo sinteza*, Moscow: Mir, 1970, vol. 3, p. 459.
- Soma, N., Nakazawa, G., Watanabe, T., Sato, Y., and Sunagawa, G., *Chem. Pharm. Bull.*, 1965, vol. 13(4), no. 3, pp. 457–464.
- Soma, N., Nakazawa, G., Watanabe, T., Sato, Y., and Sunagawa, G., *Chem. Pharm. Bull.*, 1965, vol. 13(7), no. 5, pp. 819–828.
- Metody polucheniya khimicheskikh reaktivov i preparatov* (Methods of Synthesis of Chemical Reagents and Preparations), Moscow: IREA, 1971, vol. 23, pp. 150–152.